

## Structural, magnetic and Mössbauer studies of Fe–Cu granular films

This article has been downloaded from IOPscience. Please scroll down to see the full text article.

2002 J. Phys.: Condens. Matter 14 6657

(<http://iopscience.iop.org/0953-8984/14/26/306>)

View [the table of contents for this issue](#), or go to the [journal homepage](#) for more

Download details:

IP Address: 171.66.16.96

The article was downloaded on 18/05/2010 at 12:11

Please note that [terms and conditions apply](#).

# Structural, magnetic and Mössbauer studies of Fe–Cu granular films

N H Duc<sup>1</sup>, N A Tuan<sup>2</sup>, A Fnidiki<sup>3,5</sup>, C Dorien<sup>3</sup>, J Teillet<sup>3</sup>, J Ben Youssef<sup>4</sup>  
and H Le Gall<sup>4</sup>

<sup>1</sup> Cryogenic Laboratory, Faculty of Physics, Vietnam National University, Hanoi, 334 Nguyen Trai, Thanh Xuan, Hanoi, Vietnam

<sup>2</sup> International Training Institute for Materials Sciences, 1-Dai Co Viet Road, Hanoi, Vietnam

<sup>3</sup> GPM-UMR 6634, Université de Rouen, 76821 Mont-Saint-Aignan, France

<sup>4</sup> Laboratoire de Magnétisme de Bretagne, CNRS, BP809, 29285 Brest Cedex, France

E-mail: abdeslem.fnidiki@univ-rouen.fr

Received 28 January 2002, in final form 22 April 2002

Published 21 June 2002

Online at [stacks.iop.org/JPhysCM/14/6657](http://stacks.iop.org/JPhysCM/14/6657)

## Abstract

X-ray diffraction, magnetization and Mössbauer effect investigations have been performed for the sputtered Fe<sub>0.2</sub>Cu<sub>0.8</sub> thin films. A segregation forming isolated body-centred cubic Fe grains in the face-centred cubic Cu matrix with an average diameter between 1 and 40 nm took place upon annealing in the temperature range from 100 to 500 °C. In addition, the magnetic coercive field is found to be enhanced and reaches a value of 37 mT for the sample annealed at 400 °C. A perpendicular surface anisotropy constant  $K_S = 0.04 \text{ mJ m}^{-2}$  is deduced. Surface spin configurations are discussed for the granular films investigated.

## 1. Introduction

Granular solids consisting of magnetic fine particles embedded in an immiscible medium have been intensively studied in the last decade because of the interest of their physical properties as well as their technological applications. Indeed, these materials exhibit novel phenomena such as superparamagnetism [1], giant magnetoresistance [2] and giant magnetic coercivity [1, 3].

Giant magnetic coercivity has been reported for the Fe- and Co-based granular films by several authors [1, 3–8]. The coercivity of these granular systems is as large as about 60 mT at room temperature as well as about 250 mT at  $T = 2 \text{ K}$  and is sensitive to grain size [3]. This makes these films very promising for applications—among them, as ultrahigh-density recording media. Magnetic studies of fine particles have shown that the coercivity reaches a maximum at the so-called critical diameter ( $d_c$ ) of particles and decreases as a size-inverse function ( $1/d$ ) with further increase of the diameter. The value of the effective anisotropy

<sup>5</sup> Author to whom any correspondence should be addressed.

constant,  $K_{eff}$ , estimated from the above behaviours, however, is far larger than the magneto-crystalline anisotropy for the cubic structures of the Fe- and Co-based materials. Possible factors enhancing the coercivity are:

- (i) exchange anisotropy between the metallic core and its oxide shell [9],
- (ii) magneto-elastically induced anisotropy due to large stress between the magnetic grain and the surrounding matrix [3] and
- (iii) shape anisotropy due to the deviation of the grain shape from the ideal sphere shape [4, 7].

The various approaches, however, have not so far been able to satisfactorily explain the grain size dependence of the magnetic properties in fine-particle systems.

Novel physical properties exhibited by granular materials may relate to the high density of topological defects arising at the grain surfaces. The surface atoms create a new phase and any property characteristic of this phase may become a dominant one for the whole system. Indeed, surface effects on the giant magnetoresistance were reported for Fe–Ag granular films [10]. Chen *et al* [4, 7] have also assumed that the surface anisotropy dominates the magnetic properties, including the large coercivity effect, of Fe-based granular films. Their so-called relaxation model is fairly suitable for explaining peculiarities in magnetic properties of granular systems. However, this approach seems to be imperfect in, for instance, discussing the sign of the surface anisotropy.

In this paper, we focus our attention on studying the structural and magnetic properties of the sputtered  $\text{Fe}_{0.2}\text{Cu}_{0.8}$  granular films. By processing the experimental results on the grain size dependence of the magnetic characteristics, the magnitude as well as the sign of the surface magnetic anisotropy are deduced.

## 2. Experimental details

The  $\text{Fe}_{0.2}\text{Cu}_{0.8}$  thin films were deposited on a glass substrate at 300 K by using a triode rf-sputtering system. To avoid corrosion and oxidation, the film stacks were covered with a 10 nm thick Nb layer on top. The film thickness is 380 nm. The composition was analysed using energy-dispersive x-ray spectroscopy (EDX). After deposition, samples were annealed in a vacuum of  $5 \times 10^{-5}$  Torr in the temperature range from 100 to 500 °C.

The structure of the samples was investigated by means of x-ray diffraction using a cobalt anticathode ( $\lambda_{\text{Co K}\alpha} = 0.1790$  nm). The grain size was roughly calculated from the full width at half-maximum (FWHM) of the principal diffraction peaks using Scherrer relation.

The magnetization was measured with a vibrating-sample magnetometer (VSM) in magnetic fields up to 1.4 T applied in the film-plane direction.

The conversion-electron Mössbauer spectra (CEMS) at room temperature were recorded using a conventional spectrometer equipped with a home-made helium–methane proportional counter. The source was  $^{57}\text{Co}$  in a rhodium matrix. The films were set perpendicular to the incident  $\gamma$ -beam. The spectra were fitted with a least-squares technique using a histogram method relative to discrete distributions, constraining the linewidths of each of the elementary spectra to be the same. Isomer shifts are given relatively to body-centred cubic (bcc) Fe at 300 K. The average ‘cone angle’  $\beta$  between the incident  $\gamma$ -ray direction (being the film-normal direction) and that of the hyperfine field  $B_{hf}$  (or the Fe magnetic moment direction) is estimated from the line intensity ratios 3:x:1:1:x:3 of the six Mössbauer lines, where  $x$  is related to  $\beta$  by  $\sin^2 \beta = 2x/(4+x)$ .

### 3. Experimental results and discussion

#### 3.1. Structural characteristics

The x-ray patterns are presented in figures 1(a)–(f) for the as-deposited film and films annealed at 100, 200, 300, 400 and 500 °C, respectively. For the as-deposited film, one observes five slightly broadened Bragg peaks, which can be attributed to face-centred cubic (fcc) Cu, but no bcc Fe reflections were detected. No appreciable change is observed for the annealing at  $T_A = 100$  and 200 °C. After annealing at  $T_A \geq 300$  °C, however, a clear splitting of the principal peak (around  $\theta = 26^\circ$ ) has taken place. The lower-angle peak is located at  $\theta_{\text{fcc Cu}} = 25.5^\circ$  (i.e. (111) reflections of fcc Cu) and it stays at almost the same position with increasing  $T_A$ , while the higher diffraction angle  $\theta_{\text{bcc Fe}}$  (i.e. (110) reflections of bcc Fe) slightly increases. This reflects an iron segregation from fcc (Cu–Fe) in order to form bcc Fe grains in the fcc Cu matrix. The separation of the bcc Fe (110) and fcc Cu (111) peaks becomes more visible with increasing  $T_A$ . Finally, at  $T_A \geq 400$  °C, the XRD result shows the presence of eight rather sharp peaks corresponding to five theoretical peaks of fcc Cu and three theoretical peaks of bcc Fe. This indicates a decomposition of Fe and Cu from the initial solid solution. This is consistent with the previous report by Childress *et al* [8]. The average size of bcc Fe particles ( $d_{\text{Fe}}$ ) is estimated from the FWHM using the Scherrer relation. The results obtained are listed in table 2. Note that for  $\text{Fe}_{0.2}\text{Cu}_{0.8}$  films  $d_{\text{Fe}}$  increases from 1 to 40 nm when the annealing temperature increases from 100 to 500 °C.

#### 3.2. Mössbauer spectra

The Mössbauer spectra recorded at 300 K are shown in figure 2. For the as-deposited film, the CEM spectrum consists of an asymmetric doublet (see figure 2(a)), which can be fitted fairly well as the sum of two paramagnetic subspectra: a singlet and a symmetric doublet. About 7% of the Fe atoms (table 1) were found in the singlet, characterized by an isomer shift of  $-0.09 \text{ mm s}^{-1}$ , which is typical of the austenite fcc Fe. The symmetric doublet with an isomer shift of  $0.11 \text{ mm s}^{-1}$  and a quadrupole splitting of  $0.35 \text{ mm s}^{-1}$  can be associated with Fe atoms dissolved in the fcc (Cu, Fe) phase (about 93% of the total Mössbauer fraction). These results indicate that Fe atoms dissolved in the fcc Cu phase exhibit either paramagnetic or superparamagnetic behaviour at room temperature in agreement with previous results [11]. Following annealings at  $T_A = 100$  and 200 °C, the CEM spectra are almost identical (see figures 2(b), (c)). For samples annealed at  $T_A \geq 300$  °C, besides the above-mentioned paramagnetic contributions (Fe atoms in the fcc Fe phase and Fe atoms dissolved in the fcc Cu phase), a sextet corresponding to bcc Fe ( $\delta \approx 0 \text{ mm s}^{-1}$ ,  $\langle B_{\text{hf}} \rangle \approx 33 \text{ T}$ ) is evidenced in the experimental Mössbauer spectra (see figure 2(d)). The relative bcc Fe Mössbauer fraction increases, while that corresponding to Fe atoms dissolved in fcc (Cu, Fe) phase decreases with the annealing temperature. However, it is worth noting that the total (doublet and sextet) Mössbauer fraction remains constant, i.e. always equals to about 93% of the total Mössbauer fraction. This indicated that the Fe atoms dissolved in the fcc (Cu, Fe) phase diffuse to form the bcc Fe one. In accordance with the XRD results, the increase of the relative intensity of the bcc Fe phase (see also figure 3) is associated with the evolution of the Fe grain size. In the Mössbauer spectrum for the 500 °C annealed sample, more than 80% of the Fe atoms were found in the bcc Fe phase. The remaining traces of the non-magnetic singlet and doublet in the Mössbauer spectrum indicate that the formation of bcc Fe was not complete even after annealing at 500 °C for 1 h.

The orientation of the Fe magnetic moment in bcc Fe grains can be deduced from the fitted value of the average 'cone angle'  $\langle \beta \rangle$ . This average Mössbauer angle is distributed around  $47^\circ$

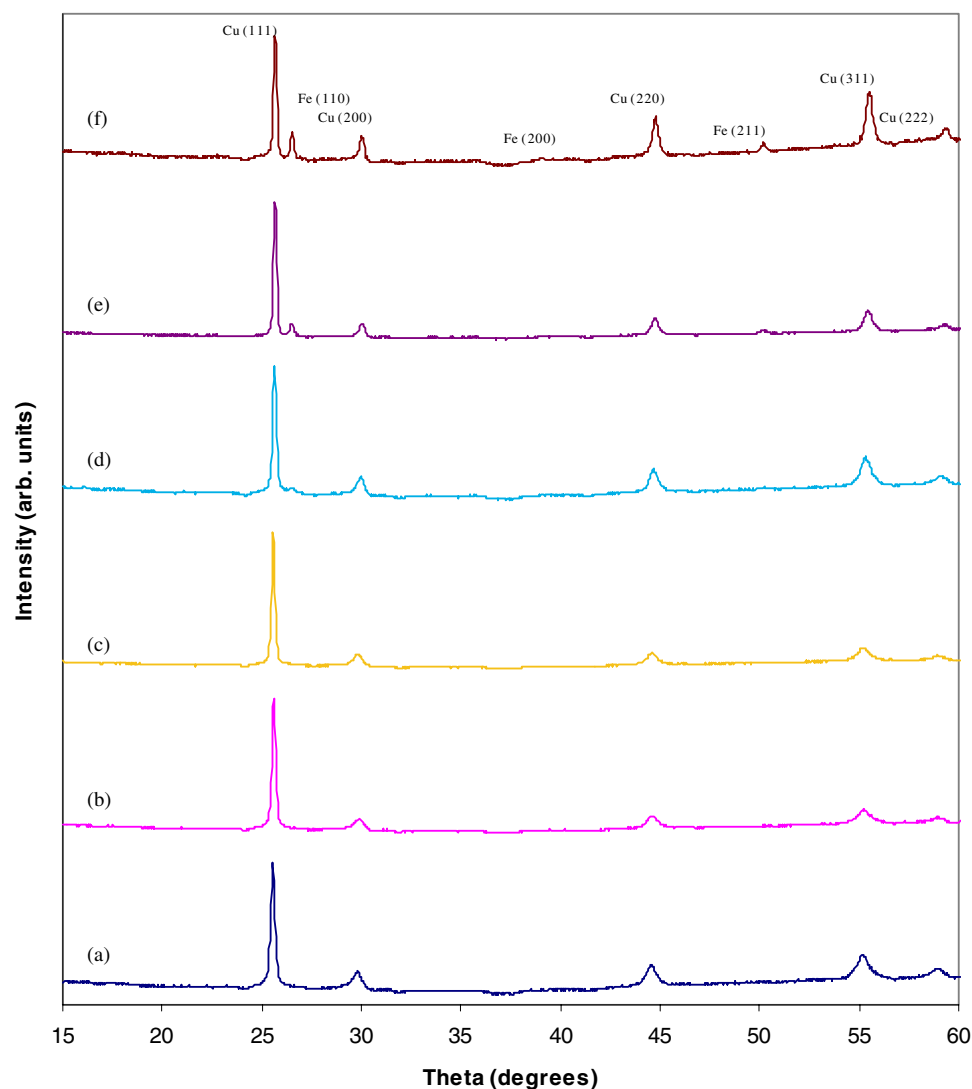


**Figure 1.** X-ray diffraction patterns of the  $\text{Fe}_{0.2}\text{Cu}_{0.8}$  thin films: (a) as-deposited film, (b) after annealing at  $100^\circ\text{C}$ , (c) after annealing at  $200^\circ\text{C}$ , (d) after annealing at  $300^\circ\text{C}$ , (e) after annealing at  $400^\circ\text{C}$  and (f) after annealing at  $500^\circ\text{C}$ .

(This figure is in colour only in the electronic version)

at  $T_A = 300^\circ\text{C}$  and seems to slightly increase with annealing temperature to around  $56^\circ$  at  $T_A = 500^\circ\text{C}$ . This value could indicate that all the spins are randomly distributed. However, if the iron spins in grain cores are assumed to be aligned in the film plane, this average orientation would imply the existence of a perpendicular magnetization component associated with the Fe/Cu interface. This notion will be supported by magnetic studies (see below) and its origin will be discussed later.

It is worth mentioning that the fcc Fe phase which was found in the Mössbauer spectra is not observed in any x-ray diffraction pattern. This is probably because its low fraction is not detectable by this technique.

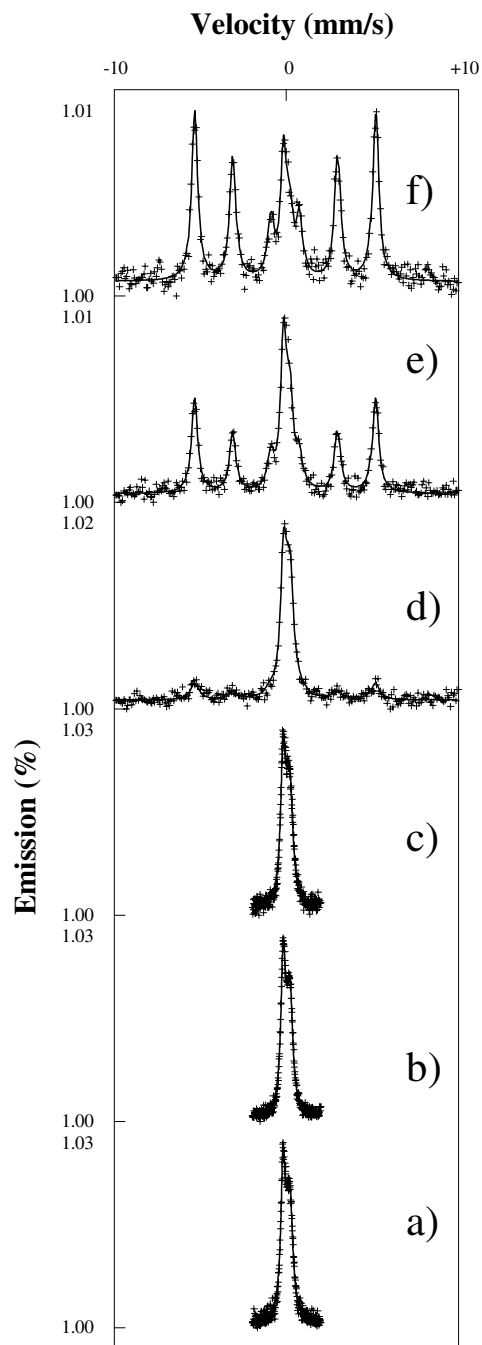


**Figure 2.** Mössbauer spectra and hyperfine-field distributions of the  $\text{Fe}_{0.20}\text{Cu}_{0.80}$  thin films: (a) as-deposited film, (b) after annealing at  $100^\circ\text{C}$ , (c) after annealing at  $200^\circ\text{C}$ , (d) after annealing at  $300^\circ\text{C}$ , (e) after annealing at  $400^\circ\text{C}$  and (f) after annealing at  $500^\circ\text{C}$ .

### 3.3. Magnetization and magnetic coercive fields

Figure 4 illustrates the magnetic hysteresis loops measured in magnetic fields applied in the film plane for the as-deposited film (i.e.  $T_A = 30^\circ\text{C}$ ) and the films annealed at  $T_A = 200, 300$  and

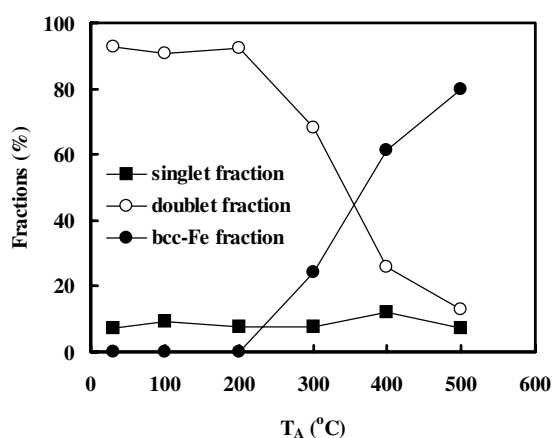


**Figure 3.** The variation of Mössbauer fractions of iron dissolved in the fcc (Cu, Fe) phase, in bcc Fe and in the fcc Fe phase for  $\text{Fe}_{0.2}\text{Cu}_{0.8}$  thin films as a function of annealing temperature.

**Table 1.** Hyperfine parameters for  $\text{Fe}_{0.2}\text{Cu}_{0.8}$  granular films: isomer shift ( $\delta$ ), quadrupolar splitting ( $\Delta$ ), hyperfine field ( $B_{hf}$ ), Mössbauer cone angle ( $\langle\beta\rangle$ ) and Mössbauer fraction ( $A$ ).

Sample, $T_A$ (°C)		$\delta$ (mm s <sup>-1</sup> )	$\Delta$ (mm s <sup>-1</sup> )	$B_{hf}$ (T)	$\langle\beta\rangle$ (deg)	$A$ (%)
30	Singlet	-0.09	—	—	—	7
	Doublet	0.11	0.35	—	—	93
100	Singlet	-0.07	—	—	—	9
	Doublet	0.11	0.37	—	—	91
200	Singlet	-0.09	—	—	—	8
	Doublet	0.11	0.34	—	—	92
300	Singlet	-0.09	—	—	—	8
	Doublet	0.11	0.34	—	—	68
	Sextet	-0.01	—	32.6	47	24
400	Singlet	-0.09	—	—	—	12
	Doublet	0.11	0.34	—	—	26
	Sextet	-0.00	—	32.7	52	62
500	Singlet	-0.09	—	—	—	7
	Doublet	0.11	0.34	—	—	13
	Sextet	-0.02	—	32.7	56	80
Accuracy		$\pm 0.02$	$\pm 0.02$	$\pm 0.1$	$\pm 5$	$\pm 2$

400 °C. The magnetic data are summarized in table 2. For the as-deposited film, the hysteresis cycle at room temperature does not show a saturation value for the magnetization, indicating that the global magnetic behaviour of the material is paramagnetic or superparamagnetic. A similar magnetic behaviour is observed for films annealed at  $T_A = 100$  and 200 °C. With further increase of the annealing temperature, the shape of the magnetic hysteresis loops evolves with saturation of the magnetization. The magnetization increases and tends to saturate at  $T_A > 300$  °C. The magnetic coercivity  $\mu_0 H_C$  initially increases with increasing  $T_A$  and reaches a maximum value of 37 mT at  $T_A = 400$  °C (figure 5). This coercivity is quite large in comparison with that for pure bcc Fe ( $\mu_0 H_C \sim 1$  mT). Upon annealing at  $T_A = 500$  °C, the coercive field decreases to 20 mT.

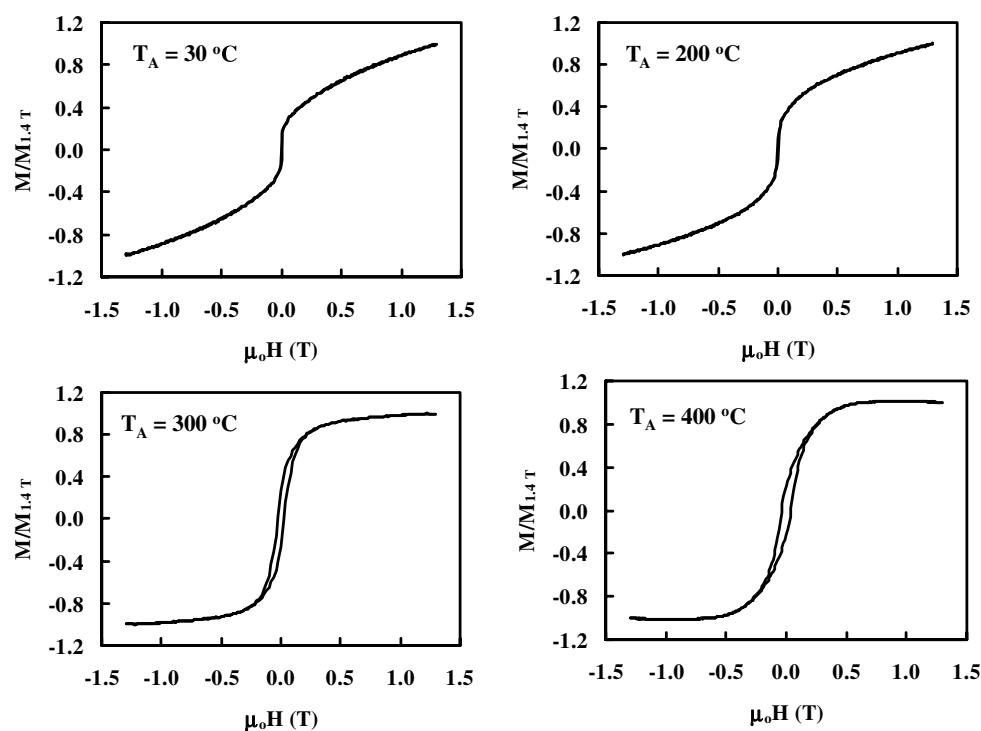


**Figure 4.** Magnetic hysteresis loops with respect to normalized magnetization  $M/M_{1.4T}$ , where  $M_{1.4T}$  is the magnetization measured for  $\mu_0H = 1.4$  T, for the  $\text{Fe}_{0.2}\text{Cu}_{0.8}$  thin films;  $T_A = 30, 200, 300$  and  $400$  °C.

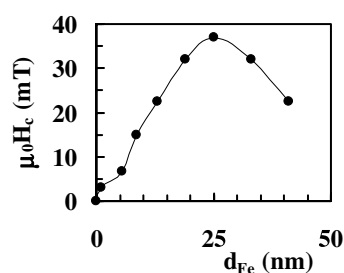


**Figure 5.** A plot of  $\mu_0H_C$  as a function of  $d_{\text{Fe}}$  for the  $\text{Fe}_{0.2}\text{Cu}_{0.8}$  thin films.

### 3.4. Surface magnetic anisotropy

According to the conventional theory, the effective magnetic anisotropy constant  $K_{eff}$  can be estimated from the coercivity  $\mu_0H_C$  and the saturation magnetization  $M_S$  using the following relation:

$$K_{eff} = \frac{1}{2}\alpha\mu_0H_C M_S \quad (1)$$

where  $\alpha$  is a constant, which depends on the magnetization reversal mechanism. According to the Stoner–Wohlfarth model, i.e. for randomly distributed single-domain particles,  $\alpha \approx 1$  (see [4] and references therein).



**Table 2.** The grain size ( $d_{\text{Fe}}$ ), magnetic coercivity ( $\mu_0 H_C$ ), saturation magnetization ( $\mu_0 M_S$ ) and effective anisotropy constant ( $d_{\text{Fe}} K_{\text{eff}}$ ) for  $\text{Fe}_{0.2}\text{Cu}_{0.8}$  granular films.

Sample, $T_A$ ( $^{\circ}\text{C}$ )	$d_{\text{Fe}}$ (nm)	$\mu_0 H_C$ (mT)	$\mu_0 M_S$ (T)	$d_{\text{Fe}} K_{\text{eff}}$ ( $\text{mJ m}^{-2}$ )
100	1	3	0.138	-0.003
200	6	6.7	0.138	-0.017
250	8.5	15	0.188	-0.111
300	13	20	0.238	-0.255
350	19	32	0.502	-0.529
400	25	40	0.502	-0.805
450	33	32	0.540	-0.718
500	41	20	0.552	-0.803

Assuming an assembly of spherical Fe fine particles with the average diameter  $d_{\text{Fe}}$ ,  $K_{\text{eff}}$  can be expressed in terms of the volume ( $K_V$ ) and surface ( $K_S$ ) anisotropy constants as [4, 7]

$$K_{\text{eff}} = K_V + 6K_S/d_{\text{Fe}}. \quad (2)$$

The enhancement of  $\mu_0 H_C$  is usually attributed to the surface contribution. With increasing  $d_{\text{Fe}}$ ,  $H_C$  first increases (for  $T_A \leq 400^{\circ}\text{C}$ ), then decreases. Thus, an assumption of a constant surface contribution may be valid for  $T_A \leq 400^{\circ}\text{C}$  only (see table 2). In figure 6, the corresponding  $d_{\text{Fe}} K_{\text{eff}}$  is plotted as a function of  $d_{\text{Fe}}$  for the domain of the linear regime for coercivity (single-domain particles). As can be seen from this figure, a large deviation from the linear variation is observed for the small grain sizes. This may be attributed, on one hand, to the stress-induced anisotropy and, on the other hand, to the variation of the surface anisotropy in the series as already indicated from the results on the Mössbauer ‘cone angle’ ( $\langle\beta\rangle$ ). For the latter reason, it is worth mentioning that the surface magnetic anisotropy depends strongly on the d-band filling as well as the nearest-neighbour geometries [12, 13]. In this context, it is the hybridization between the overlapping 3d subbands that governs the magnitude as well as the sign of the interface anisotropy [14]. Indeed, an oscillation of  $K_S$  with the d-band filling was proposed [12, 14]. At present, due to the different degree of segregation, a different modification of the band structure must be accepted for the atoms in the surface phase. We can deduce the values of  $K_V$  and  $K_S$ , approximately, from the large-grain-size region, where a sharp interface is expected to exist (because of the complete decomposition). It turns out, from this approach, that  $K_V = -40 \text{ kJ m}^{-3}$  and  $K_S = 0.04 \text{ mJ m}^{-2}$ . This finding shows that the  $K_V$ -value is rather close to that ( $-50 \text{ kJ m}^{-3}$ ) reported for the cubic anisotropy constant of pure bcc Fe [4]. The value obtained for the surface anisotropy  $K_S$  is smaller than those ( $0.4 \text{ mJ m}^{-2}$ ) reported for (Fe, Co, Ni)/ $\text{SiO}_2$  granular films [4, 7], but it is comparable with that found for (Fe, Co)/X multilayers [12]. In order to compare its magnitude with the volume magnetic anisotropy, one usually uses reduced units for the surface anisotropy,  $6K_S/d$ . Let  $d = 10 \text{ nm}$ ; we get  $6K_S/d = 25 \text{ kJ m}^{-3}$ . This simple approach, thus, is acceptable for describing the surface anisotropy contribution to the magnetic coercivity in granular films.

Although the experimental Mössbauer ‘cone angle’ ( $\langle\beta\rangle$ ) and out-of-plane magnetization data can be explained by assuming a very large surface region, one can extend the above approach to identify the negative  $K_V$  with an in-plane orientation of Fe magnetic moments in the grain core. The positive  $K_S$ , however, can be explained by two possible configurations. In the first configuration, the magnetic moments of the Fe atoms in the surface phase are along the surface normal (see figure 7(a)) and in the second one they are along the surface tangent (figure 7(b)). For both of these configurations, out-of-plane spins always exist. The value of ( $\langle\beta\rangle$ ) will be governed by the volume fraction of the in-plane and film-normal

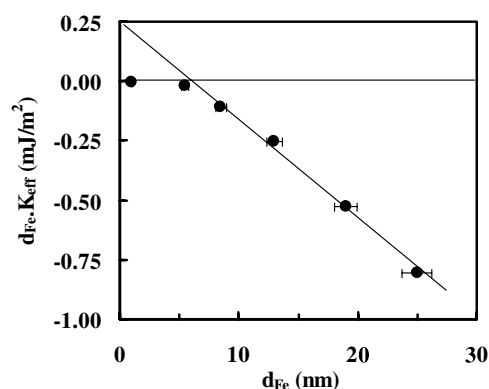


Figure 6. A plot of  $d_{Fe} K_{eff}$  as a function of  $d_{Fe}$  for the  $Fe_{0.2}Cu_{0.8}$  thin films.

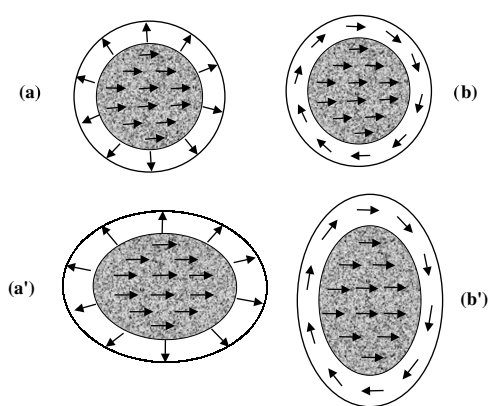


Figure 7. Surface spin configurations in granular films.

magnetization components. The indication of the perpendicular magnetization in the magnetic loops, however, depends on the shape of the fine grains. For an ideal spherical shape, the total surface magnetization is zero. The observation of the surface magnetization supports grain shapes which deviate from an ideal sphere. Furthermore, for a certain volume fraction of the surface, the perpendicular surface anisotropy can be reinforced by either oblate-like or prolate-like shape deviations as illustrated in figures 7(a') and (b'), respectively. As regards the minimization of the shape magnetic anisotropy energy, the oblate form is optimum. Indeed, it was reported by Hernando *et al* [15] that the magnetic particles tend to elongate and form larger elongated aggregates oriented along the FeCu ribbon axis. The surface spin configuration in the FeCu granular films, thus, is rather similar to that predicted for Fe/Cu multilayers [14]. So it is possible to consider the 3d(Fe)–3d(Cu) hybridization as a general mechanism of perpendicular surface anisotropy for both of these artificially nanostructured materials.

#### 4. Conclusions

The formation of the bcc Fe grains in the fcc (Cu, Fe) matrix has been evidenced by XRD, CEMS and magnetic studies on  $Fe_{0.2}Cu_{0.8}$  granular films. Enhancement of the magnetic coercivity with increasing grain size is observed. This was associated with the surface magnetic

anisotropy contribution. The magnitude as well as the sign of the surface anisotropy constant were deduced and a surface spin configuration was proposed for the FeCu granular films.

### Acknowledgment

The work of NHD and NAT is partly supported by the Programme of Fundamental Research of Vietnam, within project 420.301.

### References

- [1] Chien C L 1991 *J. Appl. Phys.* **69** 5276
- [2] Xiao J Q, Jiang J S and Chien C L 1992 *Phys. Rev. Lett.* **68** 3749
- [3] Xiao G and Chien C L 1987 *Appl. Phys. Lett.* **51** 1280
- [4] Chen C, Kitakami O and Shimada Y 1998 *J. Appl. Phys.* **84** 2184
- [5] Hayashi T, Hirono S, Tomita M and Umemura S 1996 *Nature* **381** 72
- [6] Murayama T, Miyamura M and Kondoh S 1994 *J. Appl. Phys.* **76** 5361
- [7] Chen C, Kitakami O and Shimada Y 1999 *J. Appl. Phys.* **86** 2161
- [8] Childress J R, Chien C L and Nathan M 1990 *Appl. Phys. Lett.* **50** 95
- [9] Gangopadhyay Y, Hadjipanayis G C, Dale B, Sorensen C M, Klabunde K J, Papaefthymiou V and Kostikas A 1992 *Phys. Rev. B* **45** 9778
- [10] Alof C, Stahl B, Ghafari M and Hahn R 2000 *J. Appl. Phys.* **88** 4212
- [11] Eilon M, Dong J and Street R 1995 *J. Phys.: Condens. Matter* **7** 4921
- [12] Skomski R 1998 *IEEE Trans. Magn.* **34** 1207
- [13] Gradmann U 1993 *Handbook of Magnetic Materials* vol 7, ed K H J Buschow (Amsterdam: Elsevier) pp 1–95
- [14] Givord D, McGrath O F K, Meyer C and Rothman J 1996 *J. Magn. Magn. Mater.* **157/158** 245
- [15] Hernando A, Gómez-Polo C, El Ghananami M and García Escorial A 1997 *J. Magn. Magn. Mater.* **173** 275